Image Analysis and Categorization of Ventilation-Perfusion Scans for the Diagnosis of Pulmonary Embolism Using an Expert System

Frank V. Gabor, Frederick L. Datz and Paul E. Christian

Division of Nuclear Medicine, Department of Radiology, University of Utah School of Medicine, Salt Lake City, Utah

An expert system was developed that interprets ventilation-perfusion lung scans. The use of such scans for suspected pulmonary embolism is ideal for computer-assisted diagnosis by expert systems. The data are digital, only a single disease entity is diagnosed or excluded, and well-established diagnostic criteria already exist for visual interpretation that can be easily integrated into an expert system. **Methods:** This expert system is divided into two modules. The first module is responsible for image analysis. Analysis was performed on the eight standard perfusion images and on single-breath, equilibrium and 3-min washout ventilation images. Each image was analyzed for the presence of regional perfusion or ventilation defects, as determined by pixel values that fell 2.2 s.d. below the mean (or above the mean in the case of washout images) compared with a database of normal studies. The defect size, segment involved and number of defects were determined. Ventilation and perfusion images were then compared to determine whether defects were matched or mismatched. The second program module applied the modified Biello's criteria to the data and categorized the scan as normal to low, intermediate or high probability. **Results:** A total of 80 patients were prospectively studied. An 81% (65 of 80) correlation was obtained when the results of the expert system were compared with visual interpretations made by three experienced nuclear medicine physicians. **Conclusion:** This study shows that the interpretation of ventilation-perfusion lung scans by an expert system is possible. The technique holds the promise of reducing interobserver variability and assisting less experienced observers in the interpretation of such scans.

Key Words: ventilation-perfusion scanning; expert systems; computer analysis; pulmonary embolism; artificial intelligence

J Nucl Med 1994; 35:797–802

Radionuclide ventilation-perfusion (V/Q) lung scanning is the primary imaging modality used to evaluate patients with suspected pulmonary embolism. V/Q scans are usually interpreted by human observers in two steps. First, the size and number of perfusion defects that are mismatched are determined by visual inspection of the images. Next, the findings are matched to diagnostic criteria associated with different probability levels of pulmonary embolism to categorize the scan as normal, low, intermediate or high probability.

Several sets of diagnostic criteria have been established, including those of Biello et al. (*1,2*), McNeil (*3*) and the Nuclear Medicine Working Group of the Prospective Investigation of Pulmonary Embolism Diagnosis (PIOPED) study (*1,4*). These criteria use the size, shape and number of defects seen on the perfusion images and the presence of matching ventilation and chest radiographic abnormalities to categorize scans. The criteria are designed to provide uniform interpretation of scans using prescribed algorithms. Unfortunately, significant variation occurs in V/Q interpretation among individual human observers, even when identical sets of rules are used (*5*). Variations in V/Q scan interpretation could be reduced by creating a diagnostic system that extracts purely objective data and uniformly applies diagnostic criteria. An expert system is such a system.

An expert system is designed to emulate human knowledge and decision-making processes. This is accomplished by using a set of heuristically derived rules from a human expert that are applied to the data in question. This process provides standardization of observations and decisions.

Over the last 3 yr, an expert system was developed that emulates the techniques used to interpret V/Q scans visually. The program determines the presence of perfusion defects, their size, the anatomic segments involved and the number of each size of perfusion defect. It then compares the perfusion defect data to the ventilation scan data to determine whether a V/Q mismatch exists. Finally, the data are evaluated using a set of rules based on the modified Biello et al. (*1,2*) criteria to categorize the scans as normal to low, intermediate or high probability. To the authors' knowledge, this is the first expert system developed for the analysis and interpretation of V/Q scans.

MATERIALS AND METHODS

Patient Selection

All V/Q scans performed at the University of Utah Nuclear Medicine Division over a 6-mo period were digitized. Patients

Received Sept. 7, 1993; revision accepted Dec. 20, 1993.

For correspondence or reprints contact: Frederick L. Datz, MD, Director, Division of Nuclear Medicine, Department of Radiology, University of Utah School of Medicine, 50 N. Medical Drive, Salt Lake City, UT 84132.

were excluded from the study if they were unable to complete a standard ^{133}Xe ventilation study, which included single-breath, equilibrium and washout images, or if all eight standard perfusion images could not be obtained. Patients were also excluded if chest radiographic abnormalities were present that would affect the classification of the V/Q scan.

Imaging Parameters

All images were obtained on a Picker 4/15 large-field-of-view gamma camera using a general all-purpose parallel-hole collimator (Picker Intl., Bedford Heights, OH). The camera used 61 photomultiplier tubes and a 0.25-inch thick NaI(Tl) crystal. A 20% energy window centered at the 81-keV energy peak of ^{133}Xe was used during ventilation imaging; a 20% energy window was centered at the 140-keV energy peak of ^{99m}Tc during perfusion imaging. The V/Q images were saved digitally in a 64 × 64 word format.

Ventilation images were obtained in the posterior projection using 10 mCi of ^{133}Xe. A 100,000-count single-breath image during maximal inspiration was followed by a 300,000-count equilibrium image. Subsequently, washout images were obtained at 30-sec intervals for 6 min. The single-breath, equilibrium and 3-min washout images were extracted for computer analysis.

Perfusion images were obtained following the intravenous administration of 3 mCi of ^{99m}Tc macroaggregated albumin. Imaging was performed in the posterior, anterior, left and right posterior oblique, left and right anterior oblique and left and right lateral projections. The posterior image was obtained for an information density (ID) of 3000; the remaining images were acquired for time.

Program Specifics

An expert system consisting of two modules was written in the computer language C on a Sun SPARC 2 workstation running SunOS version 4.1 (Sun Microsystems Inc., Mountain View, CA), a BSD version 4.3 compliant version of UNIX. The graphic user interface was created using version 11, release 4, of the X Window system.

The first program module extracted features from the images and analyzed the abnormalities. This required standardizing the images with respect to size and shape. Correction for anatomic variation was necessary to allow a comparison of the patient's images with a composite normal file.

To perform anatomic correction, templates of lung anatomy were created for all imaging projections. These anatomic templates represented the idealized size and shape of the lung and the segmental anatomy for each projection.

Images from each projection were subsequently stretched onto the appropriate anatomic template. First, the edge of each lung on the patient images was determined by manual outline. If a peripheral perfusion defect was present, the operator approximated the location of the lung border by continuing the outline over the defect. The amount of user interaction required was similar to that of commercially available computer-assisted diagnostic programs used in nuclear cardiology.

To be certain the manual outlining was reproducible between operators, 10 studies were processed by two different operators. The consistency of the program's final diagnosis was evaluated.

To map the image onto the template, a nonlinear stretch of the original image was performed. A plane-to-plane nonlinear mapping of images, referred to as a spatial warping function, was previously described (*6*). The spatial warping function is modeled using nth order polynomials in which the coefficients of each polynomial are estimated by selecting pairs of control points within each image.

This nonlinear stretch method first determined the center of mass of both the original image and the template to which it would be mapped. Subsequently, a radial stretch was performed, as outlined subsequently.

Both the original image of the lung and the template can be described by the radial curves

$$I(r, \theta) = 0 \quad \text{(original image)}, \qquad \text{Eq. 1}$$

$$T(r, \theta) = 0 \quad \text{(template)}, \qquad \text{Eq. 2}$$

where $\theta(x, y) = \text{atan}\ (y/x)$ and $r(x, y) = \sqrt{x^2 + y^2}$.

For a given pixel in the template $p = (x_t, y_t) = (r_t, \theta_t)$, the corresponding value in the original image is given as

$$p(x_t, y_t) = \left(\frac{1}{s_{x,y}}\right) p(x_i, y_i), \qquad \text{Eq. 3}$$

where $s_{x,y}$ is defined as the stretching factor as determined by

$$s_{x,y} = \frac{r_t}{r_i}. \qquad \text{Eq. 4}$$

The actual pixel value mapped to the template is the weighted average of the corresponding pixel values from the original image.

Next, the patient's images were compared with a normal database. The database consisted of 21 V/Q scans that had been interpreted as normal by three independent nuclear medicine physicians. The mean and s.d. were established for each pixel in all V/Q images after the images had been stretched onto the anatomic template. A value of 2.2 s.d. below the mean was defined as abnormal (in the case of the 3-min ventilation washout image, this value was defined as 2.2 s.d. above the mean). This value was empirically found to give the best trade-off between sensitivity and specificity.

To identify V/Q defects within the images, a pixel-to-pixel comparison was made between each stretched patient image and the composite normal file. Absolute counts per pixel were used. The pixel-by-pixel analysis produced a map that delineated the location of any pixels with counts below 2.2 s.d. These pixels were then submitted to a clustering criterion, which required at least two adjacent abnormal pixels to be present for an individual pixel to be classified as abnormal. In addition, a minimum size criterion of five contiguous abnormal pixels was required before an area was flagged as abnormal.

Defects were sized according to the number of contiguous abnormal pixels. Small defects were defined as being less than 30 abnormal pixels, moderate defects were between 30 and 90 abnormal pixels and large defects were greater than 90 abnormal pixels. These limits were applied to all segments. If a defect was seen on more than one view, it was sized according to its largest representation.

Ventilation abnormalities were detected in the same manner as perfusion defects, except for the washout images; these were analyzed for areas of activity more than 2.2 s.d. above the mean.

The location of the abnormal pixels in the stretched patient images was compared with the anatomic template for that view to determine the specific lung segments involved. Defects were counted only once if they involved the same segment on multiple views; this prevented overcounting of defects.

V/Q images were analyzed separately. Direct comparison of maps of V/Q abnormalities was performed to determine whether

TABLE 1
Results

		Interpretation by expert system		
		Normal to low probability	Intermediate probability	High probability
Interpretation of three nuclear medicine physicians	Normal to low probability	42	6	5
	Intermediate probability	1	8	3
	High probability	0	0	13

a perfusion defect was matched or mismatched. This could be performed only on the posterior images because ventilation images are obtained in this one projection with standard V/Q imaging.

To determine whether a V/Q mismatch was present, the posterior perfusion image was independently compared with each of the three ventilation images analyzed (single-breath, equilibrium and 3-min washout images). If the overlap of V/Q abnormalities was less than 50% of the perfusion defect's size, the defect was classified as being mismatched to ventilation.

The second program module contained the modified Biello et al. (*1,2*) criteria for diagnosing pulmonary embolism. Here, data derived from the features extraction module were evaluated using the Biello et al.'s (*1,2*) criteria to arrive at a probability for pulmonary embolism. The results were categorized as normal to low, intermediate or high probability for pulmonary embolism.

In addition to the category of pulmonary embolism (e.g., high probability), the program displayed the original images, the stretched profile of each image, a set of images with a graphic overlay of abnormal segments, the number of each size of perfusion defect and whether the defects were matched or mismatched.

To determine the accuracy of the expert system in classifying V/Q scans, the results of the computer program were compared with those of human experts. All V/Q scans entered into the study were interpreted visually by three experienced nuclear medicine physicians using the modified Biello et al. (*1,2*) criteria. In cases in which scan interpretation differed between observers, a consensus was obtained.

RESULTS

A total of 80 patients who met the patient selection criteria were entered into the study over a 6-mo period. Of these, 55 studies were visually interpreted as either normal or low probability, 12 as intermediate probability and 13 as high probability.

A comparison of the expert system's diagnoses with human experts' visual diagnoses is shown in Table 1. An 81% (65 of 80) correlation rate was achieved between the expert system and human observers. In general, the program tended to overestimate the probability of pulmonary embolism (14 of 80, 18%). Underestimation occurred in a single case (1%).

Ten V/Q scans were processed by two different operators. The expert system's final diagnosis was the same for both operators in all 10 cases.

Examples of outputs of the program are shown in Figures 1 and 2.

DISCUSSION

Scott et al. (*5*) studied the variability in the visual interpretation of V/Q scans by physicians. These investigators found a definite variation in interpretive patterns and accuracy among multiple readers of V/Q scans, despite each reader's attempt to adhere to the same diagnostic algorithm. Deviations from standard interpretive patterns were associated with diminished diagnostic accuracy. Thus, even when a well-established interpretive schema is used, variations exist in implementation among human observers.

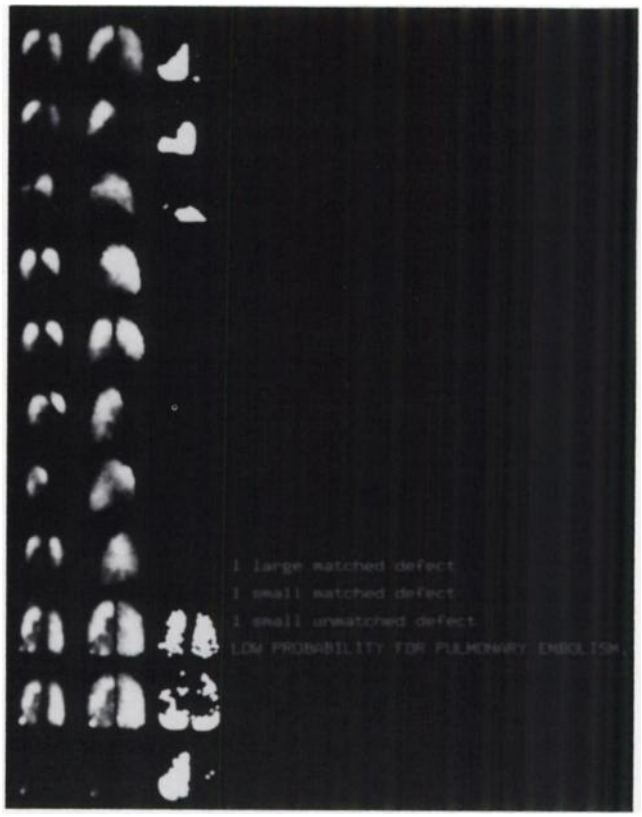

FIGURE 1. Output screen of the V/Q expert system. The left vertical column of images are the raw images. The second vertical column of images are the stretched images. The third vertical column shows perfusion and ventilation defects identified by the expert system. The text indicates the number of matched and mismatched defects and the probability of pulmonary embolism using the modified Biello et al. criteria.

FIGURE 2. Enlarged view of the left anterior oblique (LAO) image set from the output screen of a high probability scan. On the left is the raw image. In the middle is the stretched image of the left lung only. On the right is a map of the abnormal perfusion to the apical region of the lung that was identified by the expert system.

The use of an expert system for image interpretation could significantly reduce interobserver variability by objectively analyzing images and uniformly applying diagnostic algorithms. In addition, an expert system like the one described here could assist less experienced observers in the visual interpretation of V/Q scans.

To the authors' knowledge, there has only been one other fully implemented expert system in nuclear medicine. That program, developed by Ezquerra et al. (*7*) was a modification of the bull's-eye program for the diagnosis or exclusion of coronary artery disease on ^{201}Tl scans originally created by Garcia et al. (*8*). V/Q imaging for pulmonary embolism is especially well suited to computer-assisted diagnosis by an expert system because the visual diagnosis is based on a series of widely accepted rules or criteria. Thus, the diagnostic algorithm is easily defined.

Expert systems are designed to emulate the knowledge base and decision-making processes of humans in a narrowly defined domain (*9,10*). A set of heuristically derived rules is used to arrive at a decision. Expert systems are often divided into three major parts: the knowledge base, a set of decision rules and the inference engine.

The knowledge base is a special database that contains the accumulated body of knowledge, i.e., the facts and rules that experts in a particular field would possess. The decision rules are the criteria used to make the decisions. The inference engine processes the given input against the decision rules and facts of the knowledge base to derive conclusions or inferences. Decision rules can either contain firm antecedents with subsequent conclusions, or they can be based on "fuzzy" logic that allows the use of probabilistic rules and observations.

In this system, the knowledge base consisted of two parts: a database that contained a composite of normal V/Q scans and a feature extraction module that defined the existence of a defect, its size and its segmental anatomy. The decision rules consisted of computer-coded Biello et al. (*1,2*) criteria. The inference engine applied these criteria to the output of the features extraction module to make a final diagnosis.

One of the primary differences in developing an expert system for nuclear medicine compared with one in internal medicine is that, for scan interpretation, the images first must be analyzed and the features extracted. This adds a significant amount of complexity to expert systems designed for imaging compared with expert systems in other medical fields. For example, in internal medicine, the physical examination and laboratory data are acquired by a human observer and then entered into the program manually. The image analysis and feature extraction module were much more difficult to create here than the module that developed the final diagnosis.

A different potential approach to the computer-assisted diagnosis of V/Q scans is the use of neural networks. Neural networks, or parallel distributed processors, are significantly different from traditional artificial intelligence applications; they use a nonalgorithmic approach (*9–12*). This approach offers an advantage in cases in which there is a lack of well-defined rules or significant physiologic variation occurs.

Neural networks attempt to model the brain's biology by using computational units or neurons that are interconnected by weighted links. Information in the network is stored within these interconnections. Learning occurs through a series of training sets that cause an adjustment of the values of the links, thus mimicking synaptic changes in biologic systems.

Neural networks have been applied to a few areas of diagnostic radiology. Within nuclear medicine, there has been only limited application of neural networks. These include the evaluation of planar ^{201}Tl images and the diagnosis of Alzheimer's disease on PET brain scans (*13,14*). Recently, an artificial neural network was constructed for the interpretation of V/Q scans that accepted as input the visual observations of nuclear medicine physicians, such as the presence, number and size of perfusion defects (*15*). A neural network created by the authors analyzes actual images and categorizes V/Q scans, although, as yet, it can categorize scans into only two classifications (low or high probability) (*16*).

In our study, we chose to use an expert system for the computer-assisted diagnosis of V/Q scans because the interpretation of these images by humans follows a set of well-described rules (i.e., it is algorithmic in nature). Although there are various sets of diagnostic criteria for interpreting V/Q scans, an expert system can be modified relatively easily to use different diagnostic algorithms. Thus, although for the purposes of this study the modified Biello et al. (*1,2*) criteria were used, other diagnostic schemes, such as the PIOPED criteria, could have easily been applied. In fact, it would be possible to modify this program to allow the user to choose a diagnostic scheme from several different sets of diagnostic criteria.

The results of this expert system are easy for a physician to understand and confirm because the program reaches its decisions in a manner similar to that of a human expert. The size, number and location of perfusion defects and whether they are matched or mismatched are graphically displayed by the program; the rule used to make the final categorization can also be displayed. Thus, a physician can visually review the images and the diagnostic algorithm to

determine whether the visual diagnosis should be altered. This is an advantage over neural networks, which in general, do not give data as to how a particular classification was made.

This expert system was designed to interpret V/Q scans in a manner similar to that of human observers, with two exceptions. First, patients were not evaluated with chest radiographic abnormalities. To classify these patients' V/Q scans, the relative size of the infiltrate on the chest radiograph must be compared with the size of the perfusion defect on the lung scan. This would require a digital chest radiograph, which is not readily available, then construction of a second computer-assisted diagnosis program to determine the presence of an infiltrate on the chest radiograph, to size it and to compare the infiltrate's size on the chest radiograph to the relative size of the perfusion defect on the V/Q scan. Developing such a program would be a major undertaking.

A second variation of this expert system from a visual interpretation is the number of probability categories used. The normal and low probability categories were combined. This was necessary because this program frequently found a few abnormal pixels, even on scans visually read as normal. Combining these two categories can be supported from an interpretative standpoint. A low-probability scan, excluding patients with chest radiographic abnormalities, has only a 4.8% probability of pulmonary embolism, using the modified Biello et al. (*1,2*) criteria. Thus, a normal to low probability scan has a 95% probability of the patient not having pulmonary embolism. Second, data show patients with low-probability scans have an excellent prognosis. Lee et al. (*17*) followed 99 patients with low-probability V/Q scans for 6 mo; the patients were not treated with anticoagulants. None of the patients had evidence of recurrent thromboembolism or died of a thromboembolic event.

Most of the program's errors resulted in falsely overestimating the probability of pulmonary embolism. These errors in classification were primarily the result of two factors. Some cases interpreted as low probability by visual inspection were found to have diffusely abnormal perfusion scans by the expert system because of increased soft-tissue attenuation from obesity and technical factors (an ID of 3000 was not always possible in all emergency scans). Increased soft-tissue attenuation and variations from the imaging protocol have both been described as causing false-positive results with cardiac computer-assisted diagnostic programs.

The second source of error was the result of the technique used to determine whether a V/Q match or mismatch was present. A direct comparison of perfusion defects with ventilation could be performed only on the posterior images. Thus, perfusion defects that involved segments not visible on the posterior perfusion image were always considered to be unmatched. This falsely increased the probability of pulmonary embolism. Performing oblique washout images in addition to posterior images might reduce these errors by providing information about ventilatory abnormalities in more anterior lung segments.

Several other factors could decrease the program's accuracy. A potential error is the manual outlining technique. Automatic edge detection techniques are widely used in cardiac blood pool studies (*18,19*). These are based on the second derivative of the counts; the maximal rate of change in counts is defined as the edge of the ventricle. This technique would work for completely normal lung images. However, in patients with pulmonary embolism, there may be peripheral defects. In fact, centrally occurring defects surrounded by normally perfused lung, the so-called stripe sign, are unlikely to represent pulmonary emboli (*20*). An automated program would assign the proximal border of a peripheral perfusion defect as the normal lung edge; thus, the true extent of the lung would be underestimated. Previous researchers have advocated using a contour line drawn at 18% of maximum counts per pixel to produce a reliable boundary around the lung (*21*). Unfortunately, the same problem with peripheral defects also exists for this technique.

For these reasons, a manual technique was chosen to outline the lungs. Because lung outlining is an operator-dependent process, variations can occur in defining the lung edge. However, two operators outlined the lungs of 10 patients whose scans had a variety of abnormalities in this study; there was no difference between operators in the program's classification of the scans. Similar reproducibility in manual outlining has been shown with cardiac computer-assisted diagnostic programs (*8,22*). Manual outlining might not be necessary if a transmission image using a ^{99m}Tc sheet source was performed. However, transmission imaging would be time consuming because it would have to be performed on all eight standard projections and it would increase the radiation burden to the patient. For these reasons, the authors did not think that transmission images were practical.

Variation in patient positioning during imaging could also lead to errors. Although there are eight standard positions for lung perfusion imaging, as described previously, it is not always possible to obtain these at exactly the same angle in every patient. For example, the patient may be immobilized with an orthopedic device or may be unresponsive. Imprecise positioning could either hide a defect or falsely create one.

A perfusion defect may be present on multiple views of a perfusion scan. When the images are stretched onto the anatomic template, the stretch may cause a misregistration of the defect into different pulmonary segments on some views. The program would incorrectly count the single defect twice. This could falsely increase the probability of pulmonary embolism.

Several program variables were empirically set. These included the lower limit of normal of 2.2 s.d. for pixel counts, the clustering criteria of two adjacent abnormal pixels and the number of pixels used to classify defects as small, moderate or large in size. However, the use of empiric values in computer-assisted diagnostic programs is well documented in the literature; computer-assisted pro-

grams for diagnosing coronary artery disease on cardiac perfusion studies, such as the bull's-eye program and Cedars-Sinai program, use empirically derived values to differentiate normal from abnormal myocardium (*8,9,22*).

In conclusion, this study showed that the interpretation of V/Q lung scans by an expert system as an aid to visual interpretation is feasible. It holds the promise of reducing interobserver variability and assisting less experienced observers in interpreting V/Q scans.

ACKNOWLEDGMENTS

The authors thank Csaba Gabor for his help in developing the radial stretch.

REFERENCES

1. Biello DR, Mattar AG, McKnight RC, et al. Interpretation of ventilation-perfusion studies in patients with suspected pulmonary embolism. *AJR Am J Roentgenol* 1979;133:1033–1037.
2. Biello DR, Mattar AG, Osei-Wusu A, et al. Interpretation of indeterminate lung scintigrams. *Radiology* 1979;133:189–194.
3. McNeil BJ. Ventilation-perfusion studies and diagnosis of pulmonary embolism: concise communication. *J Nucl Med* 1980;21:319–323.
4. PIOPED Investigators. Value of ventilation/perfusion scan in acute pulmonary embolism—results of prospective investigation of pulmonary embolism diagnosis (PIOPED). *JAMA* 1990;263:2753–2759.
5. Scott JA, Palmer EL. Do diagnostic algorithms always produce a uniform lung scan interpretation? *J Nucl Med* 1993;34:661–665.
6. Kenny PA, Dowsett DJ, Vernon D, et al. Technique for digital image registration used prior to subtraction of lung images in nuclear medicine. *Phys Med Biol* 1990;35:679–685.
7. Ezquerra NF, Shapiro S, Garcia EV, et al. Development of an expert system for interpreting medical images. In: *Proceedings of the IEEE International Conference on Systems, Man, Cybernetics, volume* 1. New York: IEEE; 1986:205–210.
8. Garcia EV, VanTrain K, Maddahi J, et al. Quantification of rotational ^{201}Tl myocardial tomography. *J Nucl Med* 1985;26:17–26.
9. Datz FL, Rosenberg C, Gabor FV, et al. Use of computer-assisted diagnosis in cardiac perfusion nuclear medicine studies: a review (part 3). *J Digit Imaging* 1993;6:67–80.
10. Rich E, Knight K. *Artificial intelligence*, 2nd edition. New York: McGraw-Hill; 1991.
11. Boone JM, Gross GW, Greco-Hunt V. Neural networks in radiologic diagnosis: introduction and illustrations. *Invest Radiol* 1990;25:1012–1016.
12. Khanna T. *Foundations of neural networks.* Reading, MA: Addison-Wesley; 1990.
13. Rosenberg CR, Erel J, Atlan H. A neural network that learns to interpret myocardial planar thallium scintigrams. In: Giles CL, Hanson SJ, Cowan JD, eds. *Advances in neural information processing systems 5.* Palo Alto, CA: Morgan Kaufmann; 1993.
14. Kippenham JS, Barker W, Pascal S, et al. A neural-network classifier applied to PET scans of normal and Alzheimer's disease patients. *J Nucl Med* 1990(A);31:817.
15. Scott JA, Palmer EL. Neural network analysis of ventilation-perfusion lung scans. *Radiology* 1993;186:661–664.
16. Banish M, Datz FL, Clark R, et al. Application of neural networks to ventilation-perfusion imaging for diagnosing pulmonary embolism [Abstract]. *J Nucl Med* 1993;34:176P.
17. Lee ME, Biello DR, Kumar B, et al. "Low-probability" ventilation-perfusion scintigrams: clinical outcomes in 99 patients. *Radiology* 1985;156:497–500.
18. Pope DL, Parker DL, Clayton PD, et al. Left ventricular border recognition using a dynamic search algorithm. *Radiology* 1985;155:513–518.
19. Christian PE, Nortmann CA, Taylor AT. Comparison of fully automated and manual ejection fraction calculations: validation and pitfalls. *J Nucl Med* 1985;26:775–782.
20. Sostman HD, Gottschalk A. The stripe sign: a new sign for diagnosis of nonembolic defects on pulmonary perfusion scintigraphy. *Radiology* 1982; 142:737–741.
21. Burton GH, Vernon P, Seed WA. Automated quantitative analysis of ventilation-perfusion lung scintigrams. *J Nucl Med* 1984;25:564–570.
22. VanTrain KF, Maddahi J, Berman DS, et al. Quantitative analysis of tomographic stress ^{201}Tl myocardial scintigrams: a multicenter trial. *J Nucl Med* 1990;31:1168–1179.